Soft Matter

PAPER

View Article Online
View Journal | View Issue



Cite this: *Soft Matter*, 2020, **16**, 9499

# Swimming statistics of cargo-loaded single bacteria†

P. Prakash, ‡*[a] A. Z. Abdulla,§[b] V. Singh[c] and M. Varma*[ad]

Received 9th June 2020,
Accepted 19th August 2020

DOI: 10.1039/d0sm01066a

rsc.li/soft-matter-journal

Burgeoning interest in the area of bacteria-powered micro robotic systems prompted us to study the dynamics of cargo transport by single bacteria. In this paper, we have studied the swimming behaviour of oil-droplets attached as cargo to the cell bodies of single bacteria. The oil-droplet loaded bacteria exhibit super-diffusive motion which is characterised by a high degree of directional persistence. Interestingly, bacteria could navigate with cargo size as large as 8 μm resulting in an increased rotational drag of more than 2 orders when compared to the free bacteria. The directional change of cargo loaded bacterial trajectories seems to be enhanced by steric hindrance from other oil-droplets present in the environment.



## 1. Introduction

The development of micro and nano-scale robots is emerging as an intensely active area of research motivated by their applications ranging from precise drug delivery to micro-scale manipulation.[1–3] It is envisioned that bacteria-powered bio-hybrid microbots will lead to self-powered, autonomous microrobotic systems for applications in targeted delivery.[4,5] Often these microbots derive their propulsive power and navigational control externally, for instance, from an applied magnetic field.[6] The internal generation of propulsive power at microscale has been a significant challenge prompting several groups to harness the propulsive power of bacteria in developing bio-hybrid robots at microscale.[7,8] In such bacteria powered bio-hybrid microbots, a cargo, such as a polystyrene bead is transported by the collective swimming of several bacteria attached to the bead *via* chemical linkers.[9]

Previous reports of cargo attachment on bacteria have relied on attaching the cell body to very small particles (0.5–1 μm diameter) so that statistically only one cell binds due to steric restriction.[5,10] A similar chemical attachment process on the cargo with size larger than ∼10 μm yields multiple bacteria (4–10) attached to a single cargo.[11] Such an approach cannot be utilised for studying the dynamics of a single cell carrying larger loads (∼10 μm diameter). Cargo carrying single bacteria is a preferred system to undertake studies as they are devoid of complex interactions present when multiple bacteria push a single cargo. In this work, we use a sonication-based method which allows us to attach cargo to a single bacteria in the form of an oil-droplet as large as 12 μm.[12] Using oil-droplets loaded on singular bacteria we were able to study the swimming statistics of cargo carrying bacterial trajectories.

## 2. Experimental

### 2.1. Attachment of oil-droplet cargos to single bacteria

We have used the GFP (green fluorescent protein) labelled bacterial strain *Pseudomonas aeruginosa* (PA14) having one/two flagella at one end of the cell-body with average body length 1.5 ± 0.6 μm and diameter 0.6 ± 0.2 μm, respectively, in our study (Fig. 1(a)). A mixture of silicone oil (viscosity = 100 cst) and the buffer solution (0.5 mM PBS + 50 μM $MgCl_2{\cdot}6H_2O$ + 10 μM EDTA) containing bacteria (∼$10^6$ cells per mL) in a 1.5 mL Eppendorf tube was sonicated for 30–45 seconds (Fig. 1(b)). Followed by sonication, the mixture was centrifuged to separate the aqueous phase containing bacteria from the oil phase. This aqueous phase was left idle for 8–9 h, after which a fraction of bacteria in the solution was observed to be loaded with oil-droplets; see ESI† Section S1 for a detailed infographic. Due to the stochastic nature of the loading process, we observed three distinct groups of bacterial populations. There were free bacteria which were not loaded with oil-droplets, bacteria loaded with oil-droplet cargos, and bacteria were rendered

[a] *Centre for Nanoscience and Engineering, Indian Institute of Science, Bangalore, 560012, India. E-mail: praneet.iisc@gmail.com, mvarma@iisc.ac.in*
[b] *Department of Physics, Indian Institute of Science, Bangalore, 560012, India*
[c] *Molecular Reproduction, Development and Genetics, Indian Institute of Science, Bangalore, 560012, India*
[d] *Robert Bosch Centre for Cyber Physical Systems, Indian Institute of Science, Bangalore, 560012, India*

† Electronic supplementary information (ESI) available. See DOI: 10.1039/d0sm01066a

‡ Present address: Warwick Integrative Synthetic Biology Centre, University of Warwick, Coventry, CV4 7AL, UK.
§ Present address: Laboratoire de Biologie et Modelisation de la Cellule, ENS de Lyon, 69364 Lyon Cedex 07, France.

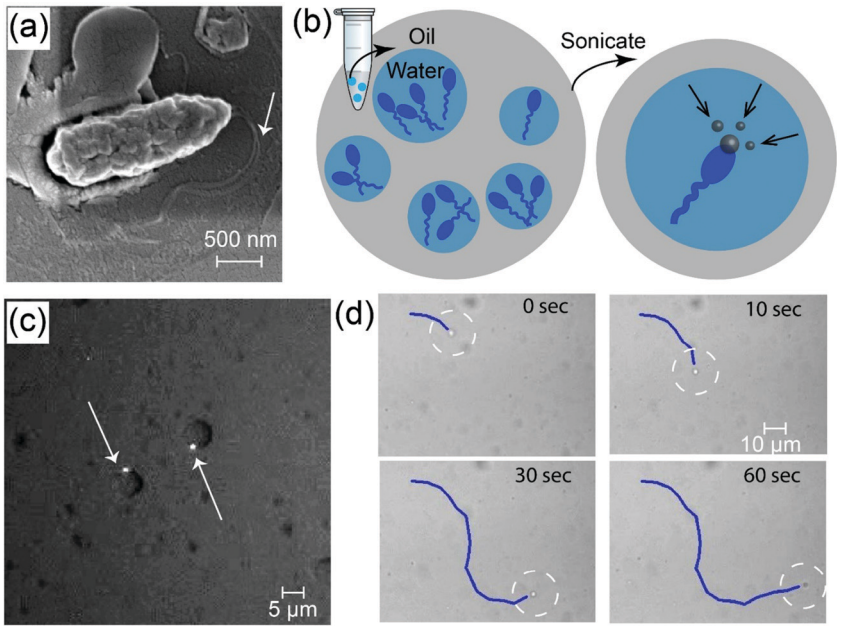


Fig. 1 (a) Scanning electron microscopy image of *Pseudomonas aeruginosa* (PA14) reveals an average length of 1.5 μm and width 0.6 μm with two flagella protruding from one end. (b) Schematic representation of loading oil-droplets on bacteria. 10 μL of bacterial solution and 200 μL of silicone oil are mixed and sonicated to load oil-droplets on bacteria. (c) Fluorescence microscopy images showing bacteria embedded onto oil-droplets. (d) Track of oil-droplets loaded on bacteria.

immobile due to large cargo size as shown in ESI,† Video S1 and the corresponding trajectories in ESI,†Video S2 (see the ESI,†for description).

### 2.2. Microscopic imaging of cargo-loaded bacteria

The aqueous phase after a maturation period of 8–9 hours was sandwiched between glass slide and cover slip separated by a sticky double tape which provides a fluidic gap of ~200 μm. Concurrent imaging near the top surface of the glass cover slip was performed using Differential Interference Contrast (DIC) and Fluorescent (FL) filters by manually switching between the two modes.[13] This allowed us to easily distinguish the GFP labelled bacterial body from oil-droplet as shown in Fig. 1(c). We recorded several oil-droplet loaded bacterial trajectories for further analysis (see ESI,†Video 3). The oil-droplet loaded bacteria can comfortably swim laterally as well as along the thickness of the flow cell as evident from variation in the focus of oil-droplet trajectory as shown in Fig. 1(d). The movies were captured at a magnification of 20× in the DIC mode after confirmation of bacterial attachment in the fluorescence mode.[14]

## 3. Results

### 3.1. Swimming speed statistics

The average swim speed of the native free bacteria taken directly from the growth medium was found to be around ~23 μm $s^{-1}$ (inset Fig. 2(a)). This is similar to the reported average swim-speed of the wild-type strain of *E. coli* bacteria, *i.e.* around ~20 μm $s^{-1}$.[15,16] Furthermore, as described in Section 2, after the cargo attachment procedure, there is still a fraction of bacterial population which is not loaded with oil-droplet cargo. We observed that the average swim-speed of these free bacteria which do not have oil-droplet cargo attached to them drops to ~15 μm $s^{-1}$ (Fig. 2(a)). The reason for this drop in the average swim-speed is probably due to nutrient deprivation during approximately 8–9 hours of a long maturation process required for the growth of oil-droplets. The bacteria loaded with oil-droplet cargos swim even slower. The swim-speed of cargo-loaded bacteria averaged over 154 tracks covering cargo diameters ranging from 2.5–12 μm was 4.3 μm $s^{-1}$ (Fig. 2(b)). The cut-off at the lower average speed of the motility data (Fig. 2(a) and (b)) is due to software limitations in tracking slow bacteria. Similarly, identification of smaller sized oil-droplets is limited by the magnification of microscope objective, which is 20× in this case (inset Fig. 2(b)). Interestingly, despite the large relative size of the oil-droplet cargo, we found this system to be quite stable and did not observe any instance of cargo detachment during our experiments. The hydrophobic nature of oil-droplet cargo and bacterial cell-membrane may account for the observed stability.[17,18]

Though *P. aeruginosa* is widely used as a model system of polar mono-flagellated bacterial species, ours is mixed mono/bi-flagellate species as revealed from the Scanning Electron Microscopy (SEM) image of our strain (Fig. 2(a); see ESI,† Section S2 for raw images). Various strains of *P.* aeruginosa are indeed reported to have more than one flagellum.[19,20] To further explore the motility behaviour, we analysed the instantaneous speed of our strain as shown in Fig. 2(c). Interestingly, the tracks exhibit meander as well as run-stop-run kind of motion, where speed drops drastically during the 'stop' events.[21] The sudden drop in the speed of bacterial species having more than one flagella such as *E. coli* is known to be the

 

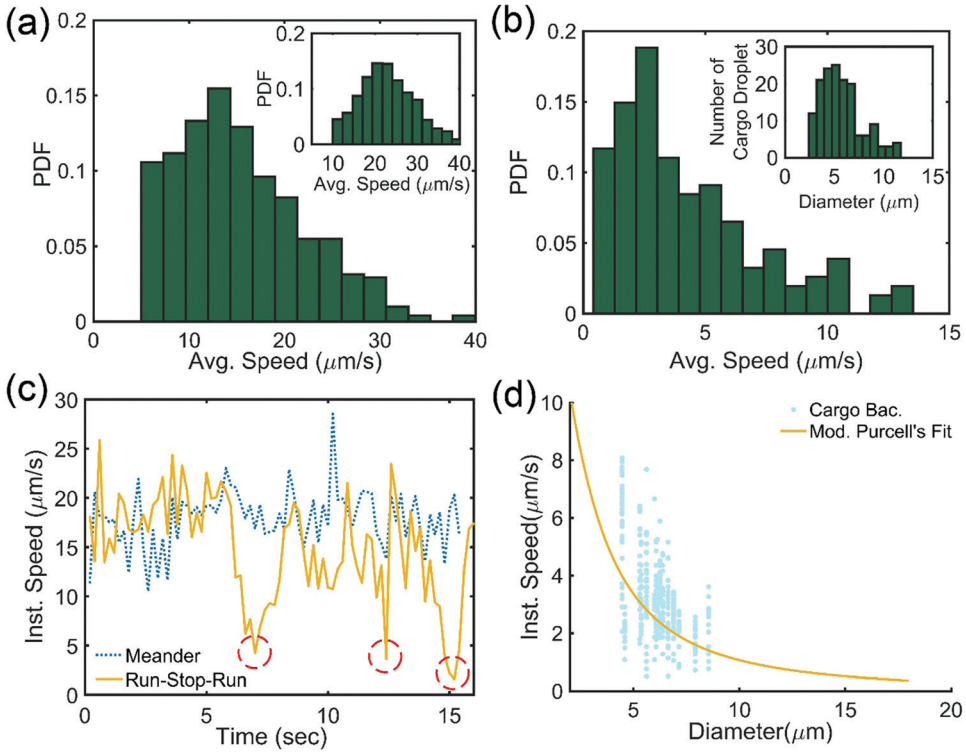


Fig. 2 (a) Average speed of starved bacteria *Pseudomonas aeruginosa* over 511 tracks is 15.3 μm $s^{-1}$. The inset shows the average speed histogram of fresh bacteria over 1814 tracks. (b) Average speed of oil-droplet loaded bacteria over 154 tracks drops to 4.3 μm $s^{-1}$. The inset image shows the histogram of the size of oil-droplets, where average size is ~6 μm. (c) Bacteria exhibit meander and run-stop-run events, where the stop events are marked when instantaneous speed drops below 5 μm $s^{-1}$. (d) Speed of cargo-loaded bacteria *vs.* size is consistent with the modified form of Purcell's model.

signature of tumbling events.[22] As oil-droplet loading process involves unconventional steps such as sonication and nutrient deprivation, we verified if the loaded bacteria indeed display wild-type motility behaviour. For analysing their motility, we modified Purcell's model to include extra drag from oil-droplet cargo as described in our recent report.[12] The speed of oil-droplet loaded bacteria is inversely proportional to the size of cargo (Fig. 2(d)) and fits well to the modified form (see extended data and derivations in Section S3, ESI†).

### 3.2. Directional persistence

A swimming bacteria performs ballistic motion for short timescales which eventually shows transition to diffusive motion for longer times.[23] Consequently, the mean-squared displacement (MSD = $\langle(r(t + dt) - r(t))^2\rangle$) of bacteria scales as $(dt)^2$ for short timescales and as $(dt)^1$ for longer timescales characterising ballistic and diffusive behaviours, respectively. The MSD of free-swimming PA14 (averaged over 41 trajectories; tracks are shown in Section S4 of the ESI†) shown in Fig. 3(a) exhibits a transition from ballistic (line with slope = 2) to diffusive behaviour (line with slope = 1) in 3.6 s. The mean-squared displacement (MSD) for diffusive motion scales with time as $\log(\mathrm{MSD}(t)) = \log(6D) + \log(t)$. Accordingly, the translational diffusion coefficient of bacteria is estimated to be 497 $\mu m^2\ s^{-1}$ from the intercept of log(MSD) *vs.* log($t$) curve using the diffusive regime (line with slope = 1) (Fig. 3(a)). The transition of bacteria from ballistic to diffusive motion can also be estimated independently from the direction auto-correlation function DACF, defined as $\mathrm{DACF}(\tau) = \langle\hat{n}(t)\cdot\hat{n}(t + dt)\rangle$, where $\hat{n}(t)$ is the unit vector in the swimming direction at time $t$. To extract the re-orientation time ($\tau_R$) of swimming bacteria, we calculated the direction auto-correlation function and fit to the exponential function $e^{-t/\tau_R}$ to obtain $\tau_R$ = 3.6 s as shown in Fig. 3(c).[24,25] One can use the reorientation timescale to estimate an effective diffusion coefficient $D_{eff}$ of bacteria swimming with an average speed of $V_0$, as $D_{eff} = V_0^2 T_R/3(1 - \alpha)$, where $T_R$ is the run duration and $\alpha$ is the mean of cosine of the re-orientation angle (see Section S5 of the ESI†).[24] The re-orientation time can be expressed as $\tau_R = T_R/(1 - \alpha)$, and accordingly, the effective diffusion can be rewritten as $D_{eff} = V_0^2\tau_R/3$.[21] Using the measured average speed of free bacteria ~15 μm $s^{-1}$, we obtain a diffusion constant of 281 $\mu m^2\ s^{-1}$ which is of the similar order as extracted from the MSD plot *i.e.* 497 $\mu m^2\ s^{-1}$. In contrast to the free bacteria, the MSD plots of cargo-loaded bacteria do not show transition to diffusive behaviour within the maximum observation window of around 90 seconds. Instead, the MSD of cargo-loaded bacteria (averaged over 16 trajectories, tracks shown in Section S4, ESI†) exhibits super diffusive behaviour with a slope of 1.8 (Fig. 3(b)). Though we cannot obtain a diffusion coefficient in the same manner as we obtained in the case of free bacteria, we can still obtain a reorientation time scale for cargo-loaded bacteria based on the DACF, which turns out to be 14.3 seconds (Fig. 3(c)). It can be noticed in the MSD plot that, this corresponds to the timescale at which the

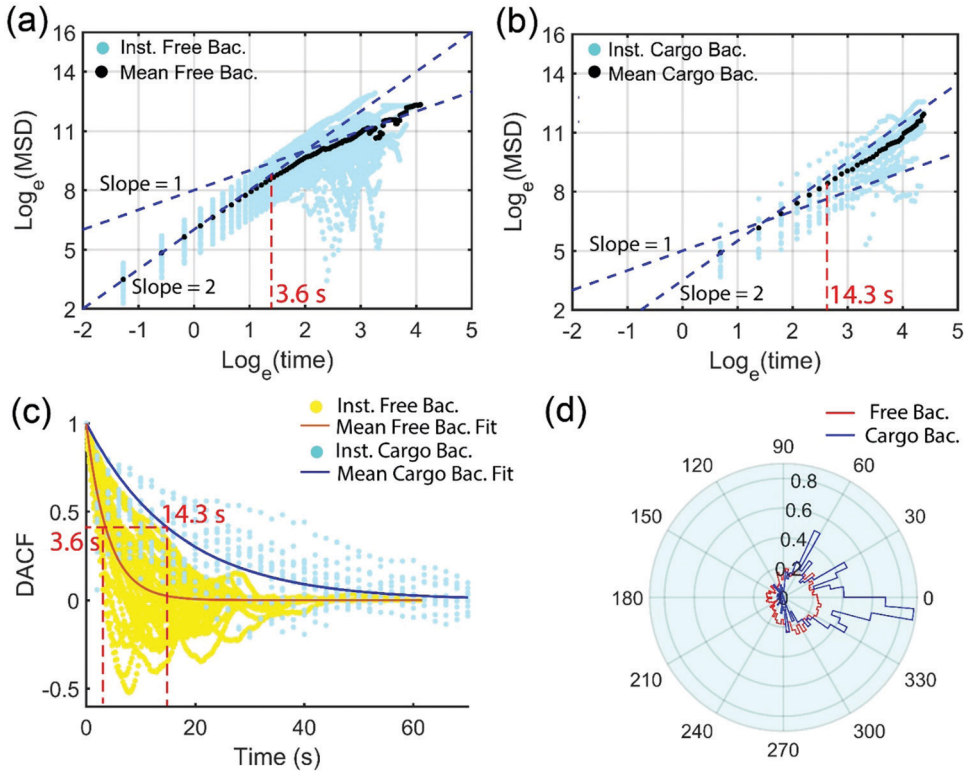


Fig. 3 Motility analysis of free and cargo-loaded bacteria. (a) MSD plot of bacteria confirms initial ballistic motion (slope = 2 on log-scale plot) which eventually becomes diffusive (slope = 1) due to tumbling events. (b) Cargo-loaded bacteria exhibit super diffusive behavior (slope $\sim$ 1.8). (c) Directional autocorrelation function shows increased persistence in the motion of cargo loaded bacteria (cyan) as compared to free bacteria (yellow). (d) Polar plot of the distribution function of bacterial orientation relative to the initial direction. Cargo-loaded bacteria proceed close to their initial direction indicating high persistence in the direction of swimming.

experimental data start deviating from the ballistic regime (line with slope = 2). The longer reorientation time of cargo-loaded bacteria translates to increased directional persistence resulting in super diffusive dynamics. This is more clearly seen when we plot the polar probability distribution function of deviation $(\theta(\tau_i) - \theta(0))$, from the initial direction $\theta(0)$, where $\tau_i$ is swept over entire track duration (Fig. 3(d)). For the oil-droplet loaded bacteria, we observe a prominent peak around the initial direction as compared to more uniformly distributed deviation in the case of free bacteria. The increased directional persistence can affect the optimum navigational strategy in porous geometries.[26–29] For instance, free bacteria exhibit diffusive motion whereas bacteria in the swarming state translocate in a super-diffusive manner similar to the cargo-loaded bacteria described here.[30]

### 3.3. Angular deviation as a function of cargo size

We have analysed the angular deviation of bacteria and cargo loaded bacteria for various time intervals ($\tau$) up to 10 s and 50 s respectively, averaged over all tracks $\theta_d(\tau) = \langle\theta(t + \tau) - \theta(t)\rangle$ as shown in Fig. 4(a). The time axis is normalised by the reorientation time for the angular deviation plot of bacteria assuming $\tau_R$ = 3.6 s, and cargo loaded bacteria assuming $\tau_R$ = 14.3 s respectively. The average angular deviation of bacterial tracks is 60° within a time interval of 12.5 s (roughly $3.5\tau_R$, $\tau_R$ = 3.6 s) whereas it is only around 30° in 50 s (roughly $3.5\tau_R$, $\tau_R$ = 14.3 s) for the oil-droplet loaded tracks (Fig. 4(a)). Clearly, the large angular deviation in bacteria leads to their transit from ballistic to diffusive behaviour which is not observed in oil-droplet loaded bacteria tracks. We then analysed the dependence of directional persistence on the size of the cargo. It is not possible to generate a large number of trajectories for a given cargo size due to the stochastic nature of the loading process. However, we get a good estimate of angular deviation by averaging over smaller time segments (40 s) from longer tracks (>50 s). Since bacteria perform random walk, an average deviation over several equidistant segments for one track is statistically as significant as the average over several trajectories. The angular deviation ($\theta_d$) of individual tracks after 40 s for oil-droplet loaded tracks as a function of their size is shown in Fig. 4(b). The error bars represent the standard error in the average change of direction after 40 s for different cargo size. Surprisingly, the angular deviation shows no significant dependence on the size of cargo for the data presented here.

### 3.4. Can we explain angular deviation by thermal or tumbling reorientations?

A change in the direction of multi-flagellated bacteria can occur either due to tumbling events or thermal diffusion. A tumbling event is distinctly identified by a sudden drop in speed, whereas

 

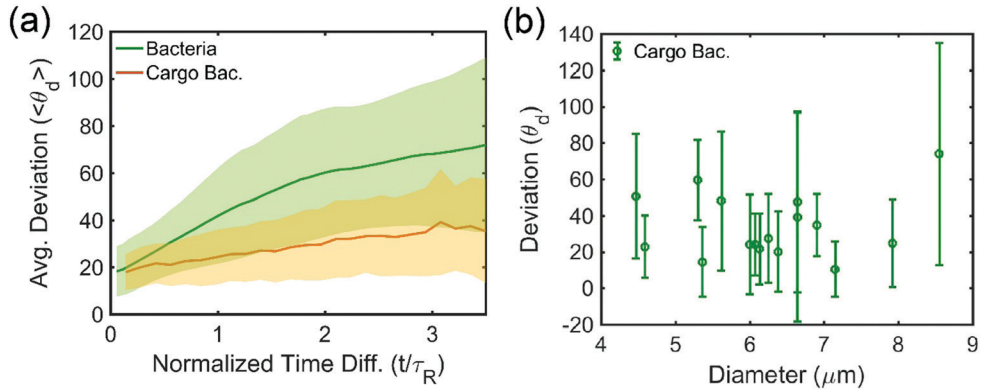


Fig. 4 (a) Angular deviation of bacteria and oil-droplet loaded tracks averaged over all tracks. The shaded area is the standard error in the angular deviation. (b) Angular deviation of oil-droplet loaded bacteria tracks *vs.* size, after 40 s. The error bar denotes the standard deviation in the change of direction after 40 s.

the reorientation due to thermal diffusion can be estimated analytically.[31] From the direct measurements of speed, we see that our strain exhibits meander as well as run-stop-run motion, as shown in Fig. 2(c). The stop event in the case of free PA14 is observed whenever there is a dip of more than 3 times in the average speed.[21] The video evidence of the tumbling event can be clearly seen in Video S1 (ESI†) where several bacterial trajectories slow down to change their direction. In particular, a sharp directional change (hallmark of tumbling events) can be noticed in trajectory 13 (a time stamp of 40 s) of the corresponding tracked movie Video S2 (ESI†).

Out of 41 free PA14 trajectories, 13 tracks underwent 2–5 stop events whereas 28 trajectories underwent either 0 or 1 stop events meaning nearly ∼68% of the total tracks are meander trajectories. The time difference between consecutive stops averaged over 13 trajectories is ∼5 s which is close to the reorientation timescale of 3.6 seconds obtained from experiments (Fig. 3(a)). Similarly, the orientation is also affected by rotational diffusion due to thermal motion. The rotational diffusion constant for free bacteria in thermal equilibrium is $D_{\mathrm{rot}} = \frac{kT}{D_{\mathrm{o}}}$, where $T$ = 300 K, with drag coefficient $D_{\mathrm{o}} = \frac{8\pi\eta_{\mathrm{w}}a^3}{3(\ln(2a/b) - 1/2)}$.[32] Considering the free bacteria as a prolate spheroid, as shown in Fig. 5(c) with $a$ = 0.75 μm and $b$ = 0.3 μm in aqueous solution with viscosity $\eta_{\mathrm{w}}$, we get $D_{\mathrm{rot}}$ = 0.3 rad$^2$ s$^{-1}$ from which the reorientation timescale can be estimated to be $\tau_{\mathrm{R}} = 1/2D_{\mathrm{rot}}$ = 1.6 s which is of the similar order of the experimentally observed value of 3.6 s. The difference in reorientation timescale is within the experimental error since the estimate is highly sensitive due to the cubic dependence of rotational drag $D_{\mathrm{o}}$ on the cell body length ($2a$ = 1.5 ± 0.6 μm). For example, if we choose '$a$ = 0.94 μm' instead of 0.74 μm which is within the error in bacterial length, then the reorientation time changes by a factor of 2. Similarly, the oil-droplet loaded trajectories also display meander and run-stop-run trajectories, as shown in Fig. 5(a). Out of 16 trajectories analysed, 4 trajectories performed run-stop-run motion where the average number of stops is ∼7 in 50 s. The average time consumed per stop in the case of cargo loaded bacteria has nearly doubled and is reminiscent of a decrease in the tumbling frequency of bacteria observed in the polymeric medium.[21] The experimentally obtained reorientation time for the cargo-loaded bacteria is ∼14.3 s which is well within the frequency of stops ∼7 s in the oil-droplet loaded bacteria. However, tumbling alone can't describe the directional change as nearly 75% of the tracks do not exhibit stop events at all. Moreover, we see no discernible pattern in the number of stops *vs.* size of cargo as shown in Fig. 5(b). As before, the reorientation time due to the thermal diffusion of oil-droplet loaded bacteria is $1/2D_{\mathrm{rot}}$, where $D_{\mathrm{rot}} = \frac{kT}{P} = 9.2 \times 10^{-3}$ rad$^2$ s$^{-1}$, $T$ = 300 K, drag coefficient $P = 8\pi\eta_{\mathrm{w}}r^3$, and average radius of oil-droplet $r$ ∼ 6 μm. As the size of cargo is much higher than the size of bacteria, the torque required for rotation is predominantly determined by the rotational drag on oil-droplets. The reorientation time scale from thermal diffusion comes out to be 55 s which is much larger than the experimentally observed value of 14.3 s. Hence, the observed independence in angular deviation as shown in Fig. 4(b) can't be explained from directional fluctuations due to thermal diffusion alone.

### 3.5 Trajectory of oil-droplet loaded bacteria

A bacterium is propelled by rotating helical flagella which couples the rotational and translational degree of freedom pushing the body forward.[33] In contrast, bacterial body and oil-droplet are symmetric, so the rotational motion of the bacterial body doesn't affect its translational motion. If the oil-droplet is attached to the head of bacteria, then it merely increases the rotational drag without having any effect on trajectory. However, if the droplet is attached to the bacterial body from sideways, as shown in Fig. 5(c), then it can alter the course of the trajectory. In such a scenario, as the bacteria move forward, the oil-droplet rotates in a forward direction as well (Fig. 5(d)). As the bacteria move forward with velocity '$V$', the angular velocity $\omega$ of the oil-droplet in the forward direction can be calculated from:

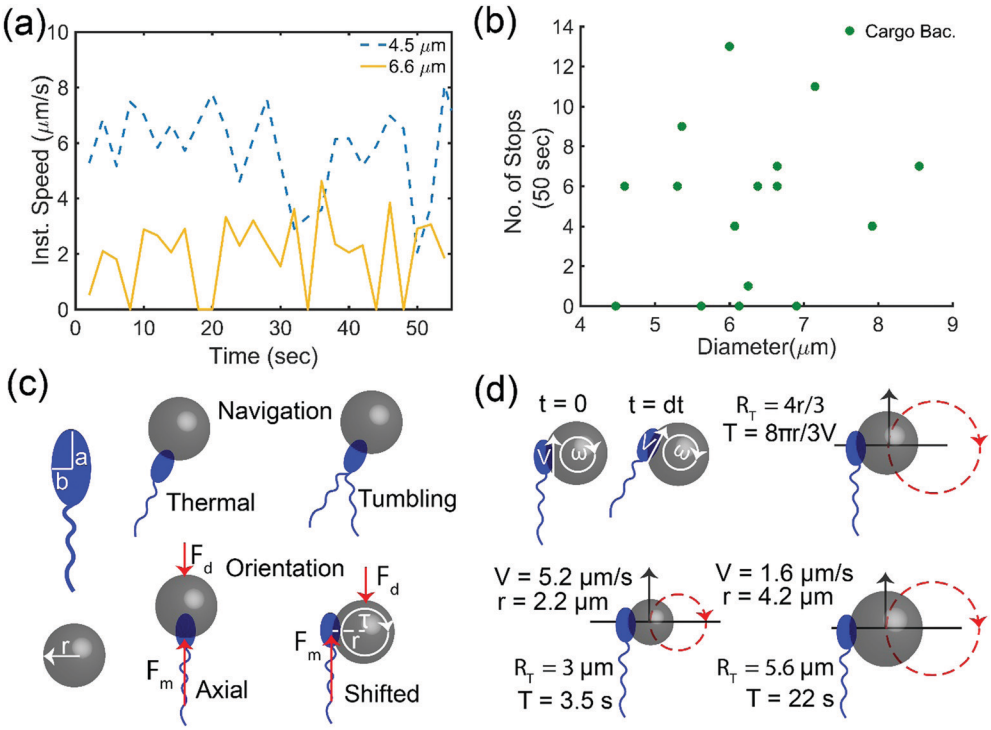


Fig. 5 (a) Cargo loaded bacteria exhibit meander and run-stop-run events. (b) Number of stops *vs.* cargo size in 50 s. (c) A schematic showing a thermal or tumbling mode of directional change. The oil-droplet attachment process is stochastic so it can attach to any part of the bacterial body. (d) If the oil-droplet is attached on the bacterial body from sideways, then it is constrained to move in circular trajectory.

$$\tau = 8\pi\eta_w r^3\omega = r \times F_m = r \times 6\pi\eta_w rV$$

where $r$ is the radius of the oil-droplet, $F_m = 6\pi\eta_w rV$ is the translational force generated by bacteria and $\eta_w$ is the viscosity of the aqueous medium. Since bacteria are always constrained to rotate on oil-droplets, the resulting trajectory will be circular. Assuming the radius of the trajectory of the oil-droplet to be $R_T$, for time '$dt$' we can write:

$$dt = R_T d\theta/V$$

By replacing $d\theta/dt = \omega = 3V/4r$, we get the radius of the trajectory as $4r/3$ and the corresponding time period $T = 8\pi r/3V$ for completing one orbit. Therefore, if the bacterial body is attached sideways, then its motion will be constrained to move in a circular trajectory with a radius 1.33 times the radius of cargo. This may seem surprising, however, because of the dynamical constraints ($\tau = r \times F_m$) an increase in velocity also results in corresponding increase of angular velocity ($\omega$) leading to a faster rotation. Hence, an increase in velocity simply results in faster rotation, consequently decreasing the time period. In our case the smallest oil-droplet is of the size of 4.4 μm and moves with a speed of 5.2 μm $s^{-1}$; therefore, if the bacteria are attached sideways, then the resulting trajectory will be of radius 3 μm. Similarly, the largest oil-droplet is of the size 8.4 μm and moves with a speed of 1.6 μm $s^{-1}$ which if attached sideways would result in a trajectory of radius 5.6 μm (Fig. 5(d)). We have seen the evidence of such trajectories in our videos, for example, see the time stamp of 5–30 s in Video S1 (ESI†) and the corresponding track 2 in Video S2 (ESI†). The time period calculation of such trajectories reveals that it would barely take 0.3 s for the smallest and 1.8 s for the largest sized bacteria to turn by an angle of 30°. This means that even a slight obstruction in front of straight trajectories can also result in a torque generation enough to quickly rotate the oil-droplet loaded bacteria. We indeed see oil-droplets attached to bacteria suddenly change their direction in the presence of stationary debris in the form of oil-droplets (see, several trajectories maneuvering through debris in Video S3, ESI†). Interestingly, this may lead to sustained angular deviation (Fig. 4(b)) even for larger sized oil-droplets as they have a higher probability of encountering debris in a littered environment.

## 4. Conclusion

To summarise, we have shown that oil-droplet loaded bacteria exhibit super diffusive motion with high directional persistence compared to the free bacteria. Interestingly, we did not observe any dependence of the cargo-size on directional persistence. This may be explained by the directional change, which occurs as the moving oil-droplet loaded bacteria encounter other stationary oil-droplets present in the system. Further experimental and corresponding theoretical analysis is required to understand the role of debris in the navigational capability of cargo loaded bacteria systems.

## Conflicts of interest

There are no conflicts to declare.

 

## Acknowledgements

P. P. was financially supported by the INSPIRE fellowship scheme of the Department of Science and Technology, Govt. of India. We thank the anonymous reviewers for their insightful comments that have significantly improved our manuscript.

## References

1 G.-Z. Yang, J. Bellingham, P. E. Dupont, P. Fischer, L. Floridi, R. Full, N. Jacobstein, V. Kumar, M. McNutt, R. Merrifield, B. J. Nelson, B. Scassellati, M. Taddeo, R. Taylor, M. Veloso, Z. L. Wang and R. Wood, *Sci. Robot.*, 2018, **3**, eaar7650.
2 B. Behkam and M. Sitti, *Appl. Phys. Lett.*, 2007, **90**, 023902.
3 A. V. Singh, Z. Hosseinidoust, B.-W. Park, O. Yasa and M. Sitti, *ACS Nano*, 2017, **11**, 9759–9769.
4 J. Bastos-Arrieta, A. Revilla-Guarinos, W. E. Uspal and J. Simmchen, *Front. Robot. AI*, 2018, **5**, 97.
5 M. M. Stanton, B.-W. Park, A. Miguel-López, X. Ma, M. Sitti and S. Sánchez, *Small*, 2017, **13**, 1603679.
6 P. Mandal, G. Patil, H. Kakoty and A. Ghosh, *Acc. Chem. Res.*, 2018, **51**, 2689–2698.
7 L. Ricotti, B. Trimmer, A. W. Feinberg, R. Raman, K. K. Parker, R. Bashir, M. Sitti, S. Martel, P. Dario and A. Menciassi, *Sci. Robot.*, 2017, **2**, eaaq0495.
8 L. Schwarz, M. Medina-Sánchez and O. G. Schmidt, *Appl. Phys. Rev.*, 2017, **4**, 031301.
9 B. Behkam and M. Sitti, *Appl. Phys. Lett.*, 2008, **93**, 223901.
10 L. Vaccari, M. Molaei, R. L. Leheny and K. J. Stebe, *Soft Matter*, 2018, **14**, 5643–5653.
11 A. V. Singh and M. Sitti, *Adv. Healthcare Mater.*, 2016, **5**, 2325–2331.
12 P. Prakash, A. Z. Abdulla, V. Singh and M. Varma, *Phys. Rev. E*, 2019, **100**, 062609.
13 G. Li and J. X. Tang, *Phys. Rev. Lett.*, 2009, **103**, 078101.
14 P. Prakash, S. Pahal and M. Varma, *Macromol. Chem. Phys.*, 2018, **219**, 1700543.
15 S. Chattopadhyay, R. Moldovan, C. Yeung and X. L. Wu, *Proc. Natl. Acad. Sci. U. S. A.*, 2006, **103**, 13712–13717.
16 V. A. Martinez, J. Schwarz-Linek, M. Reufer, L. G. Wilson, A. N. Morozov and W. C. K. Poon, *Proc. Natl. Acad. Sci. U. S. A.*, 2014, **111**, 17771–17776.
17 D. G. Allison, M. R. W. Brown, D. E. Evans and P. Gilbert, *FEMS Microbiol. Lett.*, 1990, **71**, 101–104.
18 A. Krasowska and K. Sigler, *Front. Cell. Infect. Microbiol.*, 2014, **4**, 112.
19 T. Suzuki and T. Iino, *J. Bacteriol.*, 1980, **143**, 1471–1479.
20 T. Köhler, L. K. Curty, F. Barja, C. van Delden and J. C. Pechère, *J. Bacteriol.*, 2000, **182**, 5990–5996.
21 A. E. Patteson, A. Gopinath, M. Goulian and P. E. Arratia, *Sci. Rep.*, 2015, **5**, 15761.
22 L. Turner, W. S. Ryu and H. C. Berg, *J. Bacteriol.*, 2000, **182**, 2793–2801.
23 H. C. Berg, *E. coli in Motion*, Springer, New York, 2004.
24 P. S. Lovely and F. W. Dahlquist, *J. Theor. Biol.*, 1975, **50**, 477–496.
25 K. Martens, L. Angelani, R. Di Leonardo and L. Bocquet, *Eur. Phys. J. E: Soft Matter Biol. Phys.*, 2012, **35**, 84.
26 T. Jakuszeit, O. A. Croze and S. Bell, *Phys. Rev. E*, 2019, **99**, 012610.
27 P. Prakash and M. Varma, *Sci. Rep.*, 2017, **7**, 15754.
28 A. T. Brown, I. D. Vladescu, A. Dawson, T. Vissers, J. Schwarz-Linek, J. S. Lintuvuori and W. C. K. Poon, *Soft Matter*, 2016, **12**, 131–140.
29 P. Prakash, A. Z. Abdulla and M. Varma, *arxiv*, 2020.
30 G. Ariel, A. Rabani, S. Benisty, J. D. Partridge, R. M. Harshey and A. Be'er, *Nat. Commun.*, 2015, **6**, 8396.
31 J. Saragosti, P. Silberzan and A. Buguin, *PLoS One*, 2012, **7**, e35412.
32 H. C. Berg, *Random walks in biology*, Princeton University Press, 1993.
33 E. M. Purcell, *Proc. Natl. Acad. Sci. U. S. A.*, 1997, **94**, 11307–11311.